Submandibular adenoid cystic carcinoma presenting with liver metastasis as the initial symptom: A case report

TIANYI LI[1], TINGYAO MA[1], YUE ZHAO[1], SHUJING ZHANG[1], GUOLIANG YANG[1], XUELIAN WANG[1], XUDONG WANG[1], MINGZHU WANG[1], XI ZHAO[1], HONGFEI LIU[1], JUN WU[1], XIAOLI ZHAO[2,3] and XIAOHONG CHEN[1]

[1]Department of Otolaryngology-Head and Neck Surgery, Beijing Tongren Hospital, Capital Medical University, Beijing 100730, P.R. China; [2]Department of Pathology, Beijing Tongren Hospital, Capital Medical University, Beijing 100730, P.R. China; [3]Beijing Key Laboratory of Head and Neck Molecular Diagnostic Pathology, Beijing 100730, P.R. China

Received April 9, 2025; Accepted August 29, 2025

DOI: 10.3892/ol.2025.15342

Abstract. Adenoid cystic carcinoma (ACC) is a rare and aggressive malignancy characterized by a high incidence of distant metastasis. However, cases of ACC with liver and lymph node metastases are rarely reported and lack a standardized treatment consensus. The present report describes the case of a submandibular gland ACC with liver metastasis manifesting as the initial symptom. PET/CT revealed masses in the left submandibular gland and the liver. The patient underwent right tri-lobe hepatectomy and resection of the submandibular gland tumor. Histological examination of the tumor revealed a cribriform type with both lymphovascular invasion and perineural invasion. New lymph node metastases were observed 21 months after surgery of the submandibular gland tumor, and no further treatment was administered to date. The patient has survived for 28 months since the diagnosis of liver metastasis and currently exhibits stable vital signs. In conclusion, the present case illustrates a rare, high-risk variant of rapidly progressing submandibular gland ACC, with liver metastasis serving as the initial presenting symptom. A multidisciplinary approach is essential for the effective management of complex metastatic ACC.

Correspondence to: Professor Xiaohong Chen, Department of Otolaryngology-Head and Neck Surgery, Beijing Tongren Hospital, Capital Medical University, 1 Dong Jiao Min Xiang Street, Dongcheng, Beijing 100730, P.R. China
E-mail: trchxh@163.com

Dr Xiaoli Zhao, Department of Pathology, Beijing Tongren Hospital, Capital Medical University, 1 Dong Jiao Min Xiang Street, Dongcheng, Beijing 100730, P.R. China
E-mail: zhaoxl710@sina.com

Key words: head and neck cancer, adenoid cystic carcinoma, liver metastasis, submandibular gland

Introduction

Adenoid cystic carcinoma (ACC) is a rare and aggressive malignancy, comprising only ~1% of head and neck malignancies (1) and ~10% of salivary gland tumors (2). Most ACC cases arise from the minor salivary glands, with the palate and sinuses identified as the most common sites. A smaller proportion of cases originate from the major salivary glands, primarily the parotid gland (3-5). ACC is characterized by its indolent growth, lymphovascular invasion, perineural invasion and a high incidence of distant metastasis. The long-term prognosis for patients with ACC is poor, with a 10-year overall survival (OS) rate of ~50%. Age >50 years, T3-4, N+, M1, presence of lymphovascular invasion, perineural/nerve invasion and positive/close margin status are significant predictors for decreased survival (6). Notably, distant metastases occur in 40-50% of cases, and the median survival time following metastasis is <3 years (7). Common metastatic sites include the lungs, liver and bones, with lung metastases being the most frequent, comprising 56-85.9% of metastases, whereas lymph node metastases are very rare (6,8). Initial treatment most commonly consists of surgery with adjuvant radiation for the primary site (9), but there is no consensus on the management of liver metastases. The present report describes a rare case of submandibular gland ACC with liver metastasis as the initial clinical manifestation, and summarizes relevant literature to provide insights into the diagnosis and management of rapidly advancing high-risk ACC.

Case report

A 69-year-old female patient presented at Beijing Tongren Hospital (Beijing, China) in February 2022 with a complaint of paroxysmal colicky pain in the mid-abdomen for a duration of 3 weeks. Abdominal CT revealed multiple irregularly shaped hepatic masses, the largest measuring ~15.7x14.3 cm (Fig. 1). Cancer antigen 19-9 levels were recorded as 41.8 U/ml (reference range: 0-37 U/ml), whereas α-fetoprotein, carcinoembryonic antigen and other tumor biomarkers were negative. PET/CT imaging was performed to assess both local and systemic lesions, revealing a mildly hypermetabolic mass in

the left submandibular gland, hypermetabolic lymph nodes in the left upper deep neck and multiple hepatic masses exhibiting unevenly increased metabolism (Fig. S1); these findings were highly suggestive of malignancy.

Following the exclusion of contraindications, a right tri-lobe hepatectomy and regional lymph node dissection were performed at Beijing Youan Hospital (Beijing, China) in April 2022. Pathological analysis revealed multiple hepatic tumors, the largest measuring ~19x14x10 cm, featuring a firm, gray-white cross-section (data not shown). All specimens were fixed in 4% neutral buffered formalin at room temperature for 24 h within 30 min of devitalization, then grossed and subjected to routine dehydration, clearing and paraffin embedding. Next, 4 μm sections were obtained from each paraffin block using a microtome (MICROM HM 340E; Thermo Fisher Scientific, Inc.) and stained with hematoxylin-eosin (HE). Samples were de-waxed in two changes of xylene (5 min each), rehydrated to water with graded alcohols and stained with hematoxylin for 5 min. After washing the sections in water, the samples were differentiated in 1% hydrochloric acid in 70% ethanol. Sections were stained with eosin for 3 min, re-immersed in alcohol and xylene, dehydrated in ethanol, cleared in xylene and cover slipped in a resinous mountant. Under an Olympus BX53 upright microscope, tumor cells were observed to be arranged in tubular, cribriform and cord-like patterns, comprising epithelial and myoepithelial cell components (Fig. 2). Based on the clinical history, the findings were indicative of ACC with multiple liver metastases. Moreover, genomic profiling was performed by Genetron Health (Beijing, China) using a hybridization-capture-based targeted panel and Illumina high-throughput sequencing. Genetic testing identified 15 gene mutations, including ATP binding cassette subfamily C member 8, A-kinase anchoring protein 10, α kinase 1, BCL6 corepressor, carnosine synthase 1, cyclin dependent kinase inhibitor 1C, DEAF1 transcription factor, lysine demethylase 4B, keratin associated protein 17-1, matrix metallopeptidase 24, phosphoinositide-3-kinase regulatory subunit 1 (PIK3R1), solute carrier family 12 member 2, SOX10, spermatogenesis and centriole associated 1 like and spectrin α, erythrocytic 1 (Table I); three gene copy number variations involving Achaete-Scute family BHLH transcription factor 2, forkhead box L2 and NK2 homeobox 1; no gene rearrangements; microsatellite stability; and a tumor mutational burden of 0.49 mutations/mb.

After 3 months, the patient sought further diagnosis and treatment for an anterior neck mass at Beijing Tongren Hospital. This had been identified 6 years prior on the left anterior neck and measured ~1 cm, without any apparent pain, breathing difficulties, swallowing problems, choking or hoarseness. Initially disregarded, the mass had recently exhibited gradual enlargement. MRI of the neck revealed a nodular lesion in the posterior region of the left submandibular gland, displaying slightly prolonged T1 and T2 signals with heterogeneous intensity, a high signal on diffusion-weighted imaging and apparent diffusion coefficient, and measuring ~3.3x2.3x3.4 cm. The lesion appeared lobulated with indistinct boundaries and demonstrated notable heterogeneous enhancement on contrast-enhanced scans (Fig. 3). Enlarged lymph nodes were observed in the left cervical level II region. Ultrasonography revealed an irregular hypoechoic lesion in the

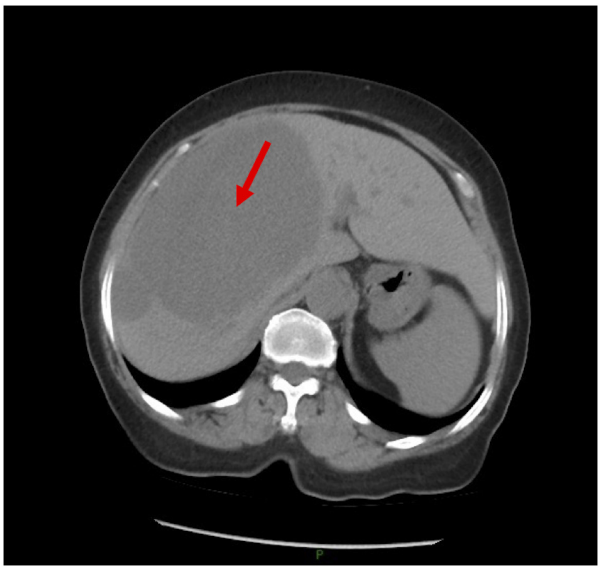

Figure 1. Abdominal CT image showing multiple liver lesions.

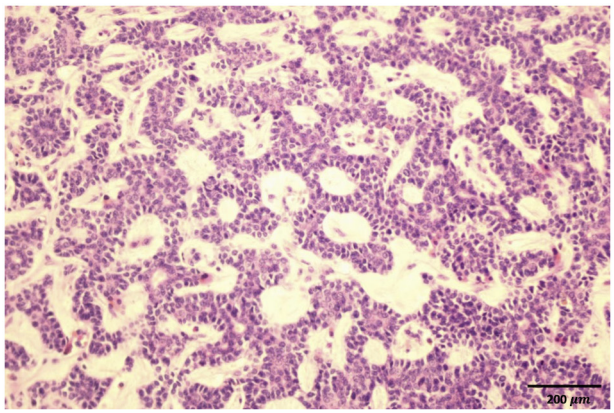

Figure 2. Histological image of liver metastasis in adenoid cystic carcinoma showing tumor cells arranged in tubular and cribriform patterns (H&E stain; magnification, x200).

left submandibular area with well-defined margins, protruding into the subcutaneous tissue, exhibiting heterogeneous internal echoes, scattered calcifications and minimal blood flow signals both around and within the lesion (Fig. 4).

Following the exclusion of contraindications, the patient underwent resection of the submandibular gland tumor and cervical lymph node dissection at Beijing Tongren Hospital (Beijing, China) in July 2022. Pathological examination following surgery revealed a grayish-white, hard mass in the submandibular gland, measuring ~4.5x2.5x3.2 cm (data not shown). HE staining was performed as described above. The tumor was microscopically diagnosed as ACC, exhibiting primarily cribriform structures (80%), with tubular (15%) and solid (5%) patterns, demonstrating high differentiation without high-grade transformation. Lymphovascular invasion and perineural invasion were observed; one lymph node exhibited metastasis, with the largest metastatic focus measuring ~2 mm and exhibiting extranodal extension (Fig. 5). Immunohistochemical staining was performed with the envision two step method. All primary antibodies

Table I. Detected gene mutations and potential clinical significance.

Gene	Protein function	Clinical significance
ABCC8	Modulator of ATP-sensitive potassium channels and insulin release	Mutations have been associated with non-insulin-dependent diabetes mellitus type II and hyperinsulinemic hypoglycemia of infancy
AKAP10	Differentially targeted protein that binds to type I and II regulatory subunits of protein kinase A and anchors them to the mitochondria or the plasma membrane	Polymorphisms in this gene may be associated with increased risk of arrhythmias and sudden cardiac death
ALPK1	Serine/threonine-protein kinase that detects bacterial PAMPs	Associated diseases include retinal dystrophy, optic nerve edema, splenomegaly, anhidrosis and migraine headache syndrome
BCOR	An interacting corepressor of BCL6, a POZ/zinc finger transcription repressor may influence apoptosis	BCOR is altered in several solid and hematologic malignancies including acute myeloid leukemia and kidney clear cell sarcoma
CARNS1	Catalyzes the formation of carnosine and homocarnosine	Associated diseases include Persian Gulf syndrome
CDKN1C	A strong inhibitor of several G1 cyclin/CDK complexes and a negative regulator of cell proliferation	Mutations in this gene are implicated in sporadic cancers and Beckwith-Wiedemann syndrome
DEAF1	A zinc finger domain-containing protein that functions as a regulator of transcription	Associated diseases include neurodevelopmental disorder with hypotonia and impaired expressive language and with or without seizures
KDM4B	Enables histone H3K36 demethylase activity and histone H3K9me2/H3K9me3 demethylase activity	Biomarker of several diseases, including alopecia areata, lung cancer, medulloblastoma, prostate cancer and stomach cancer
KRTAP17-1	KAP proteins form a matrix of keratin intermediate filaments which contribute to the structure of hair fibers	Associated diseases include limited scleroderma
MMP24	Breakdown of extracellular matrix	Associated diseases include cerebral arteriopathy, autosomal dominant, with subcortical infarcts and leukoencephalopathy, type 1 and Waardenburg syndrome, type 2E
PIK3R1	This gene encodes the regulatory subunit of PI3-kinase. PI3-kinase phosphorylates the inositol ring of phosphatidylinositol at the 3' position	Mutated in several cancers, most frequently in glioma, endometrial and colorectal cancers
SLC12A2	The protein encoded by this gene mediates sodium and chloride transport and reabsorption	Associated diseases include Delpire-Mcneill syndrome and Kilquist syndrome
SOX10	A transcription factor involved in embryonic development and cell fate	SOX10 amplification has been identified in several cancers, including melanoma, bladder cancer and nasopharyngeal carcinoma
SPATC1L	Predicted to be involved in spermatogenesis	Associated diseases include spermatogenic failure 16 and male infertility due to acephalic spermatozoa
SPTA1	The encoded protein is primarily composed of 22 spectrin repeats which are involved in dimer formation. It forms a component of the erythrocyte plasma membrane	Mutations in this gene result in several hereditary red blood cell disorders

The information presented in this table is available in the GeneCards (https://www.genecards.org/) and OncoKB (https://www.oncokb.org/) databases. ABCC8, ATP binding cassette subfamily C member 8; AKAP10, A-kinase anchoring protein 10; ALPK1, α kinase 1; PAMPs, pathogen-associated molecular pattern metabolites; BCOR, BCL6 corepressor; POZ, poxvirus and zinc finger; CARNS1, carnosine synthase 1; CDKN1C, cyclin dependent kinase inhibitor 1C; DEAF1, DEAF1 transcription factor; KDM4B, lysine demethylase 4B; KRTAP17-1, keratin associated protein 17-1; KAP, keratin-associated protein; MMP24, matrix metallopeptidase 24; PIK3R1, phosphoinositide-3-kinase regulatory subunit 1; SLC12A2, solute carrier family 12 member 2; SOX10, SRY-box transcription factor 10; SPATC1L, spermatogenesis and centriole associated 1 like; SPTA1, spectrin α, erythrocytic 1.

were purchased from Beijing Zhongshan Golden Bridge Biotechnology Co., Ltd. (OriGene Technologies, Inc.) in a ready-to-use format, including Calponin (cat. no. ZA-0524; clone EP63), CD117 (cat. no. ZA-0523; clone EP10), cytokeratin (CK; cat. no. ZM-0069; clone AE1/AE3), CK7 (cat. no. ZM-0071; clone UMAB161), CK8/18 (cat. no. ZM-0315;

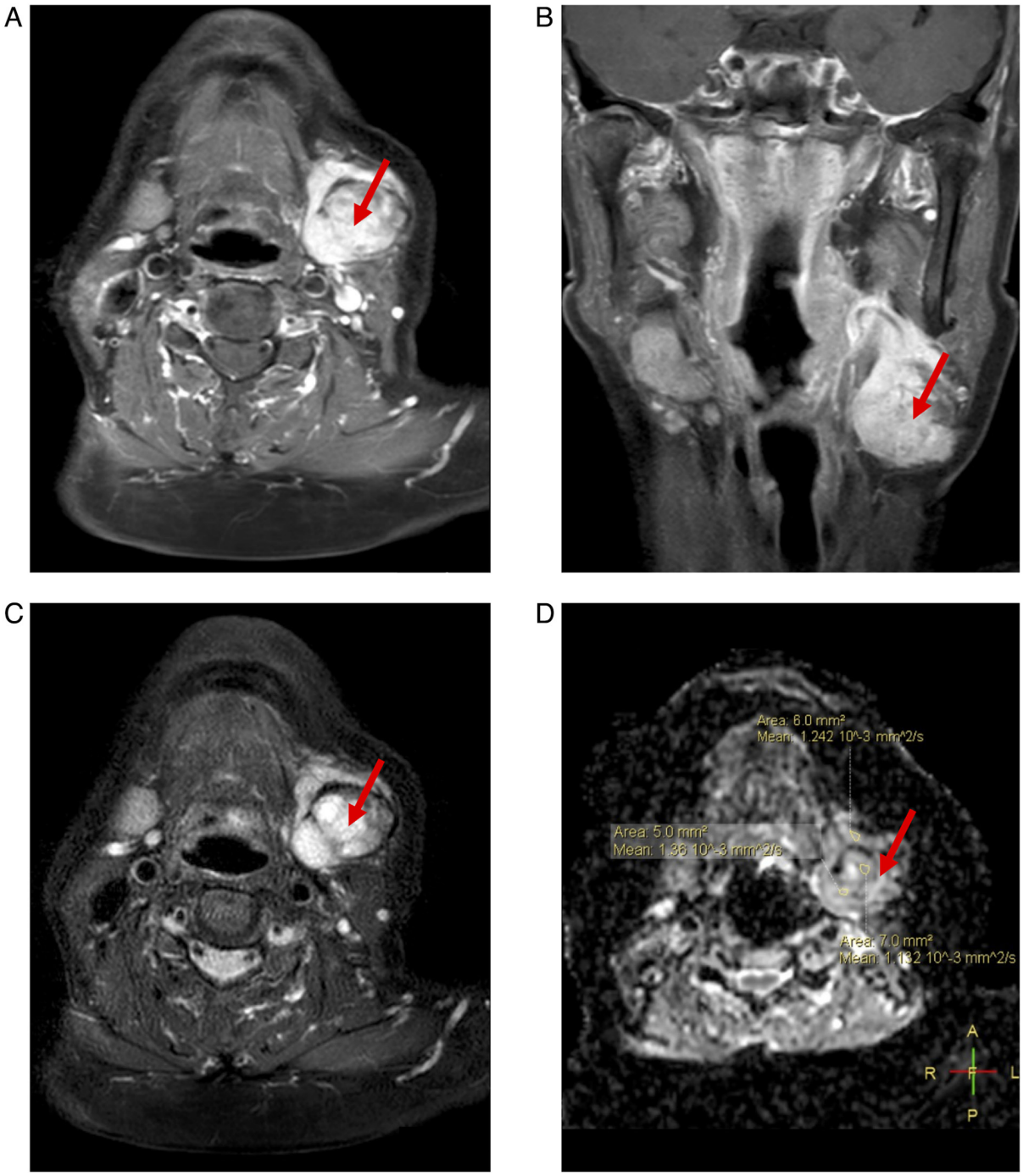

Figure 3. Cervical MRI. Nodular lesion in the (A) horizontal and (B) coronal plane with slightly elongated T1 and (C) long T2 signals in the left submandibular gland region, with (D) high signal on diffusion-weighted imaging.

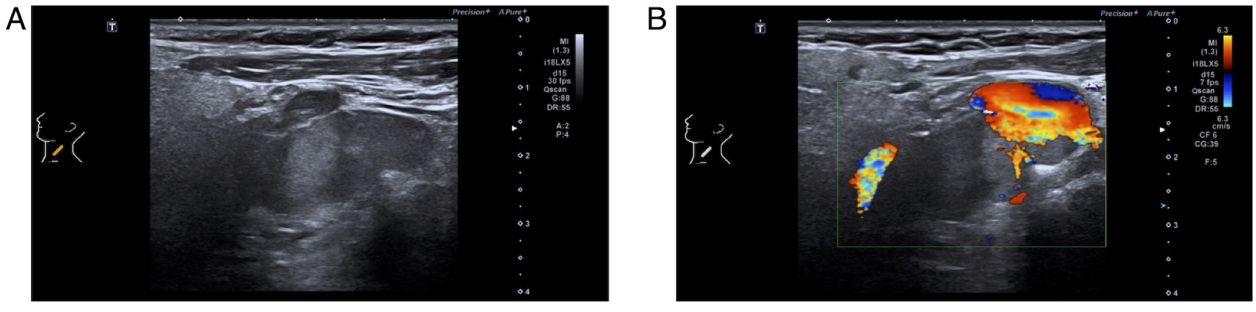

Figure 4. Preoperative color Doppler ultrasound of the salivary glands and draining lymph nodes. (A) Irregular hypoechoic mass in the left submandibular area, with (B) sparse blood flow signals around and within the lesion.

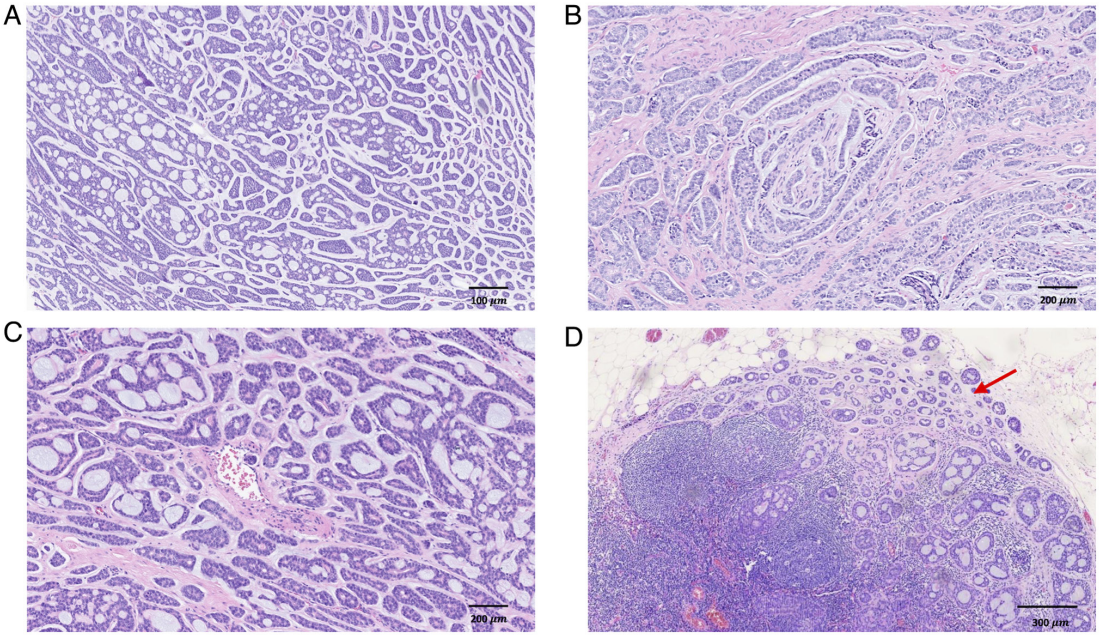

Figure 5. Histological image of submandibular gland adenoid cystic carcinoma (hematoxylin-eosin stain). (A) Predominantly composed of cribriform structures (80%), with tubular (15%) and solid (5%) patterns, demonstrating high differentiation without high-grade transformation (magnification, x100). (B) Perineural invasion and (C) lymphovascular invasion were observed (magnification, x200). (D) Lymph node exhibited metastasis exhibit extranodal extension (magnification, x40).

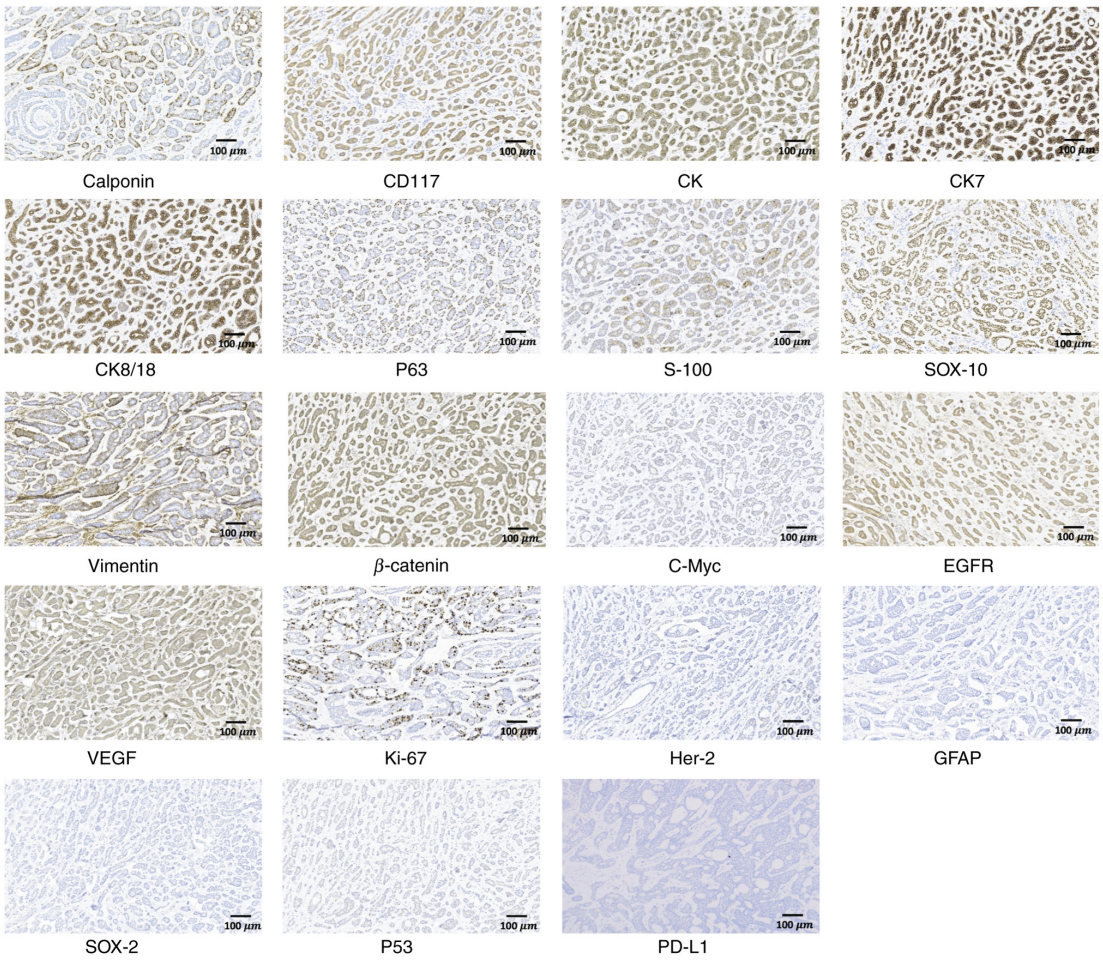

Figure 6. Immunohistochemical images of submandibular gland adenoid cystic carcinoma, revealing positive expression of Calponin, CD117, CK, CK7, CK8/18, P63, S-100, SOX-10, Vimentin, β-catenin, C-Myc, EGFR, VEGF, and Ki-67 index in hot-spot (10-15%), alongside negative expression of Her-2, GFAP, SOX-2, P53 and PD-L1 (magnification, x100). CK, creatine kinase; CK7, cytokeratin 7; CK8/18, cytokeratin 8/18; SOX, SRY-box transcription factor; GFAP, glial fibrillary acidic protein; PD-L1, programmed death-ligand 1.

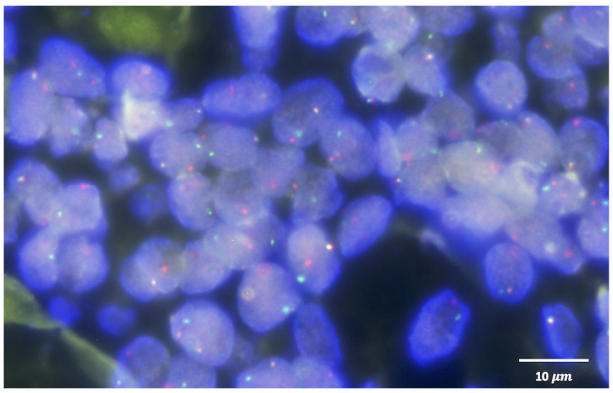

Figure 7. *MYB* gene rearrangement was not detected by fluorescence *in situ* hybridization in the primary adenoid cystic carcinoma (magnification, x1,000).

clone B22.1 and B23.1), p63 (cat. no. ZA-0553; clone B18), S-100 (cat. no. ZM-0224; clone 15E2E2 and C4.9), SRY-box transcription factor (SOX)10 (cat. no. ZA-0624; clone EP268), Vimentin (cat. no. ZM-0260; clone UMAB159), β-catenin (cat. no. ZM-0442; clone UMAB15), C-Myc (cat. no. ZA-0555; clone EP121), EGFR (cat. no. ZM-0093; clone UMAB95), VEGF (cat. no. ZA-0287), Ki67 (cat. no. ZM-0166; clone UMAB107), Her-2 (cat. no. ZM-0065; clone UMAB36), GFAP (cat. no. ZM-0118; clone UMAB129), SOX-2 (cat. no. ZA-0571; clone EP103), p53 (cat. no. ZM-0408; clone DO-7) and PD-L1 (cat. no. ZA-0629; clone SP142). Tissue sections were deparaffinized and rehydrated. Antigen retrieval was achieved by pressure cooking in 0.1 M citrate buffer pH 6 for 10 min followed by cooling at room temperature. The endogenous peroxidase was inactivated with 3% hydrogen peroxide for 10 min. Sections were pre-incubated with 10% goat serum (cat. no. E07-100, OriGene Technologies, Inc.) at room temperature for 30 min to block non-specific antibody binding. Subsequently, the sections were incubated overnight at 4˚C with specific primary antibodies followed by horseradish peroxidase-linked goat anti-mouse/rabbit secondary antibody (cat. No. TA373082/TA373083; 1:500; OriGene Technologies, Inc.) at room temperature for 60 min. Controls were carried out by omitting the primary antibody. The reactions were visualized by 3,3-Diaminobenzidine. The slides were then counterstained with hematoxylin as aforementioned and mounted using a synthetic resin. Immunohistochemical analysis under an Olympus BX53 upright microscope revealed positive expressions of Calponin, CD117, creatine kinase, CK7, CK8/18, P63, S-100, SOX10, Vimentin, β-catenin, C-Myc, EGFR, VEGF, Ki67 index in hot-spot (10-15%), alongside negative expression of Her-2, glial fibrillary acidic protein, SOX-2, p53 and programmed death-ligand 1 (PD-L1) (Fig. 6). MYB fluorescence *in situ* hybridization (FISH) was carried out on 4-μm formalin-fixed paraffin-embedded sections using an Anbiping MYB break apart probe (cat. no. F.01247-01; Guangzhou Anbiping Pharmaceutical Technology Co., Ltd.). After deparaffinization, rehydration and heat-mediated antigen retrieval (100˚C, 25 min), tissue was digested with proteinase K (37˚C, 15 min) to enhance probe penetration, dehydrated and air-dried. Slides were co-denatured with the MYB break-apart probe (red 455 kb 5'/green 577 kb 3') at 85˚C for 5 min, hybridized overnight at 37˚C, stringency-washed with saline sodium citrate buffer and then counterstained with DAPI at room temperature for 10 min. Signals were scored under a fluorescence microscope with appropriate single-band filters. FISH analysis of the primary ACC tumor specimen revealed no MYB gene rearrangement (Fig. 7).

A total of 4 months following liver metastasis surgery, a new lesion in the left hepatic lobe was identified (data not shown) and treated with ultrasound-guided percutaneous microwave ablation, resulting in a successful surgical outcome and recovery. Follow-up concluded at the end of May 2024, by which time cervical lymph node metastasis in the left level Ib and II regions (Fig. 8) and multiple hepatic masses were observed. The patient declined any additional interventions due to concerns of pain and treatment burden. Subsequent follow-ups were unsuccessful despite repeated contact efforts.

Discussion

ACC is a rare malignant tumor that represents ~1% of all head and neck cancer cases and ~10% of salivary gland malignancies. ACC characteristically grows slowly, with a 5-year OS rate of 68-90%. Long-term outcomes indicate that the 10- and 15-year OS rates decrease to 52 and 28%, respectively, with neural invasion, failure of local control and distant metastasis identified as the primary causes (4). Distant metastasis occurs in 16.1-72.7% of cases, typically within ~8 years post-treatment but earlier in salivary gland ACC (10,11). The most common metastatic sites are the lungs, followed by bones, the liver and the brain (12).

ACC of the head and neck with liver metastasis is infrequently documented and lacks a standardized treatment consensus. To date, only seven cases of ACC with liver metastasis as the initial clinical manifestation have been documented, to the best of our knowledge (13-19) (Table II). Most of these cases identified the submandibular gland as the primary site, with liver metastasis potentially occurring in both early- and late-stage patients based on tumor (T) staging. Only Spolverato *et al* (16) and the patient described in the present report exhibited simultaneous lymph node metastasis, to the best of our knowledge.

Beyond the clinical rarity, the propensity for submandibular ACC liver metastases may be related to anatomical location, lymph node metastases and molecular alterations. Patients with submandibular gland ACC exhibit a notably higher rate of neck lymph node metastasis and distant metastasis within the first year of diagnosis, as well as more rapid disease progression, compared with those with parotid gland ACC (20). Furthermore, lymph node involvement may increase the risk of distant metastasis. Lymph node metastasis is infrequent in ACC, with a rate of ~17% in the salivary gland (21). The patient in the current report presented with positive lymph node metastasis and was classified as being at a locally advanced stage; therefore, selective neck lymph node dissection was performed. Patients with advanced-stage submandibular gland ACC have a markedly lower survival rate in comparison with those with ACC located in other regions (22). Critically, molecular alterations may also drive metastasis. The patient had EGFR and VEGF upregulation and a *PIK3R1* mutation. PI3K signaling serves an important role in cancer cell survival, angiogenesis and metastasis (23). A previous study reported

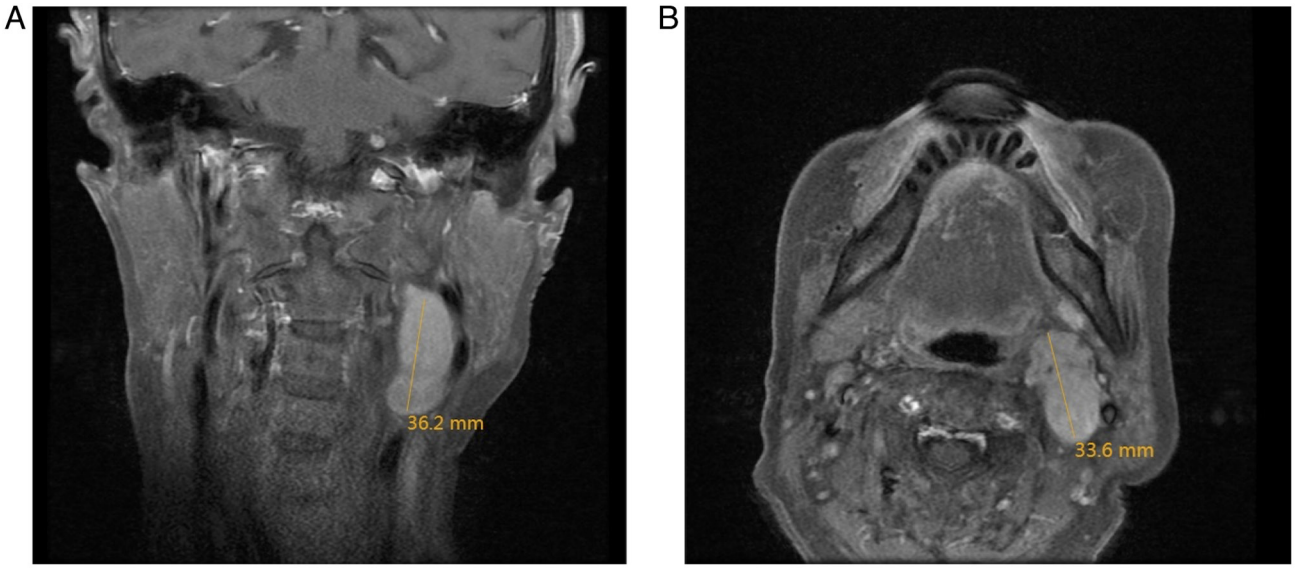

Figure 8. Cervical MRI enhancement in the (A) coronal and (B) horizontal plane showing a heterogeneous and markedly enhanced mass in the left cervical level Ib and II regions.

that inhibitors of EGFR and PI3K/AKT could suppress the proliferation, migration and neural invasion of SACC-83 cells (24). Collectively, the anatomical predisposition, nodal metastasis and activation of pro-metastatic pathways may have converged to drive the occult distant metastasis and rapid progression observed in the present submandibular ACC case.

Upon initial examination, an ultrasound revealed multiple liver lesions in the patient in the present report. To further evaluate the local and systemic condition, PET/CT was performed, revealing a metabolically increased mass in the left submandibular gland. The diagnosis of multiple liver metastases originating from left submandibular gland ACC was confirmed through a combination of clinical examination, imaging studies, biopsy and postoperative histopathological analysis. The patient tested negative for *MYB* gene breakage and rearrangement, and the absence of the ACC-specific molecular marker, *MYB-NFIB*, removed a key molecular diagnostic clue.

The patient was diagnosed with both submandibular gland ACC and liver metastases, necessitating distinct therapeutic approaches for the primary site and the liver metastases. Whilst no specific treatment consensus exists for head and neck ACC with multiple liver metastases, hepatectomy for liver metastases originating from other malignancies has been recognized as an effective treatment modality (25). Given the substantial size of the liver tumor, which had already invaded the right lobe, continued tumor growth could have resulted in liver failure. The patient had a favorable evaluation of liver reserve, with a remnant liver volume to standard liver volume ratio of ~57%, indicating potential surgical tolerance. Consequently, a right hepatectomy was performed to address the liver metastasis prior to excising the primary tumor. The primary tumor was subsequently treated in accordance with American Society of Clinical Oncology guidelines, which recommend surgery combined with postoperative radiotherapy as the optimal strategy for localized ACC (26). Research suggests that patients with advanced submandibular gland ACC derive the most benefit from adjuvant radiotherapy (22). The surgical and postoperative radiotherapy regimen was adopted; however, the patient discontinued standard postoperative radiotherapy due to perceived pain during treatment, which may have contributed to local recurrence 21 months post-surgery.

Particle radiotherapy, chemotherapy, targeted therapy and immunotherapy may offer survival benefits and enhance the quality of life for patients with ACC experiencing local recurrence and refractory distant metastasis (7). The PD-L1 immunohistochemical result of the patient in the present case was negative, indicating that the patient was not eligible for treatment with immune checkpoint inhibitors as part of a novel immunotherapy approach. However, the patient tested positive for EGFR and VEGF, permitting consideration of targeted therapies such as cetuximab, lapatinib and pazopanib. An earlier study involving patients with ACC indicated that cetuximab treatment in a cohort of 23 individuals did not yield a meaningful response; however, 12 patients experienced disease stabilization for >6 months (27). Another study involving 19 patients with advanced ACC reported no response to lapatinib; however, 15 patients experienced disease stabilization for ≥6 months (28). Furthermore, in a clinical trial involving 46 patients treated with pazopanib, only one case demonstrated a partial response, with a median progression-free survival of 5.9 months and OS of 16.6 months (29). Genetic testing of the patient in the present case indicated that the mutations clustered in genes associated with cell growth and developmental disorders (such as *CDKN1C*, *BCOR*, *PIK3R1* and *SOX10*). Among the mutated genes, *PIK3R1* was the only gene associated with potential clinical targeted therapies (30), although its clinical efficacy in patients with ACC remains unclear.

In conclusion, to the best of our knowledge, the present case represents the sixth report in the literature in which submandibular gland ACC initially manifests with atypical liver metastasis as the first symptom, without involvement of other common metastatic sites. The present case demonstrates a rare, high-risk variant of rapidly progressing ACC, with liver metastasis serving

Table II. Literature review of adenoid cystic carcinoma presenting with liver metastasis as the initial symptom.

First author/s, year	Age, years	Sex	Primary site	Initial presentation	Stage	Histopathological characteristics	Imaging features (liver metastasis)	Management	Follow-up	(Refs.)
Walker *et al*, 2025	29	Male	Parotid gland	Right upper quadrant abdominal pain and early satiety	T4N0M1	Tubiform and cribriform	A bulky mass (left lobe, 14 cm)	TACE, chemotherapy and radiotherapy	Alive with disease after 5 months	(13)
Brincat and Cassar, 2024	50	Female	Submandibular gland	Asymptomatic	pT1N0	Tubiform and cribriform	Solitary (left lobe)	Primary excision + SND (IA and IB) + locoregional radiotherapy; and left lateral liver sectionectomy (liver segments II/III)	No recurrence after 4.5 years	(14)
Li *et al*, 2021	51	Female	Sublingual gland	Asymptomatic	NA	Tubiform and cribriform; MYB-NFIB fusion positive	Solitary (right lobe)	Partial right hepatic lobectomy and primary excision	Recurrence after	(15)
Spolverato *et al*, 2014	59	Female	Submandibular gland	Mild, vague abdominal pain	T3N2bM1	Solid architecture with certain areas characterized by a cribriform pattern; t(6;9)(q22-23; p23-24)	Solitary	Extended left hepatectomy with concomitant lymphadenectomy; and primary excision + ND + adjuvant systemic therapy	No recurrence after 5 months	(16)
Garg *et al*, 2014	75	Male	Submandibular gland	Pain and a lump in the right hypochondrium associated with loss of appetite and weakness	NA	NA	Multiple (both lobes)	Treatment declined	NA	(17)

Table II. Continued.

First author/s, year	Age, years	Sex	Primary site	Initial presentation	Stage	Histopathological characteristics	Imaging features (liver metastasis)	Management	Follow-up	(Refs.)
Karatzas *et al*, 2011	51	Female	Submandibular gland	Asymptomatic	NA	NA	Multiple (both lobes)	TACE + atypical extended right hepatectomy with right liver lobe and segment IVA liver resection; intraoperative RFA (segment II); and percutaneous RFA (segment III)	No recurrence after 1 year	(18)
Deshpande and Kelkar, 2009	68	Male	Submandibular gland	Weight loss, an upper abdominal lump, and itching all over the body	NA	NA	Multiple (both lobes)	Chemotherapy declined	NA	(19)
Present study	69	Female	Submandibular gland	Paroxysmal colicky pain in the mid-abdomen	T3N2bM1	Cribriform structures (80%) with tubular (15%) and solid (5%) patterns	Multiple (right lobe)	Right hepatectomy; RFA; and primary excision + SND	Alive with disease after 28 months	-

T, tumor stage; N, node stage; M, metastasis stage; pT, pathological T stage; TACE, transcatheter arterial chemoembolization; SND, selective neck dissection; ND, neck dissection; RFA, radio frequency ablation; NA, not available; NFIB, nuclear factor I B.

as the initial presenting symptom. Immunohistochemistry and genetic testing may facilitate the identification of novel therapeutic strategies, including immunotherapy and targeted therapy, beyond traditional chemotherapy and radiotherapy. Moreover, a multidisciplinary approach is essential for the effective management of complex metastatic ACC.

Acknowledgements

Not applicable.

Funding

The present study was supported by the National Natural Science Foundation of China (grant nos. 82173312 and 82372967) and Capital's Funds for Health Improvement and Research (grant no. 2022-2-2057).

Availability of data and materials

The data generated in the present study may be requested from the corresponding author.

Authors' contributions

TL was a major contributor to the conception of the study, as well as to the literature search for related studies. TM and XLW were involved in the literature review, study design and obtaining medical images. YZ, MW, XZ and XDW were involved in the processing of the figures and analyzing patient data. SZ, GY, HL and JW participated in the clinical discussion and patient management. XLZ and XC contributed to the acquisition and interpretation of data. XLZ and XC confirm the authenticity of all the raw data. All authors have read and approved the final version of the manuscript.

Ethics approval and consent to participate

The present study was performed in accordance with the Declaration of Helsinki, and approved by the Ethics Committee of Beijing Tongren Hospital, Capital Medical University (approval no. TREC2022-KY023).

Patient consent for publication

Written informed consent was obtained from the participant for the publication of the details of the medical case and any accompanying images.

Competing interests

The authors declare that they have no competing interests.

References

1. Spiro RH, Huvos AG and Strong EW: Adenoid cystic carcinoma of salivary origin. A clinicopathologic study of 242 cases. Am J Surg 128: 512-520, 1974.
2. Ciccolallo L, Licitra L, Cantú G and Gatta G; EUROCARE Working Group: Survival from salivary glands adenoid cystic carcinoma in European populations. Oral Oncol 45: 669-674, 2009.
3. Bjørndal K, Krogdahl A, Therkildsen MH, Overgaard J, Johansen J, Kristensen CA, Homøe P, Sørensen CH, Andersen E, Bundgaard T, *et al*: Salivary gland carcinoma in Denmark 1990-2005: A national study of incidence, site and histology. Results of the Danish head and neck cancer group (DAHANCA). Oral Oncol 47: 677-682, 2011.
4. Atallah S, Casiraghi O, Fakhry N, Wassef M, Uro-Coste E, Espitalier F, Sudaka A, Kaminsky MC, Dakpe S, Digue L, *et al*: A prospective multicentre REFCOR study of 470 cases of head and neck adenoid cystic carcinoma: Epidemiology and prognostic factors. Eur J Cancer 130: 241-249, 2020.
5. Coca-Pelaz A, Rodrigo JP, Bradley PJ, Vander Poorten V, Triantafyllou A, Hunt JL, Strojan P, Rinaldo A, Haigentz M Jr, Takes RP, *et al*: Adenoid cystic carcinoma of the head and neck-An update. Oral Oncol 51: 652-661, 2015.
6. Ouyang DQ, Liang LZ, Zheng GS, Ke ZF, Weng DS, Yang WF, Su YX and Liao GQ: Risk factors and prognosis for salivary gland adenoid cystic carcinoma in southern China: A 25-year retrospective study. Medicine (Baltimore) 96: e5964, 2017.
7. Nightingale J, Lum B, Ladwa R, Simpson F and Panizza B: Adenoid cystic carcinoma: A review of clinical features, treatment targets and advances in improving the immune response to monoclonal antibody therapy. Biochim Biophys Acta Rev Cancer 1875: 188523, 2021.
8. van Weert S, Bloemena E, van der Waal I, de Bree R, Rietveld DH, Kuik JD and Leemans CR: Adenoid cystic carcinoma of the head and neck: A single-center analysis of 105 consecutive cases over a 30-year period. Oral Oncol 49: 824-829, 2013.
9. Dalal P, Dermody S, Brummel C, Brenner C, Casper K, Chinn SB, Malloy KM, Mierzwa ML, Neal MH, Prince MEP, *et al*: Clinical outcomes in salivary adenoid cystic carcinoma. J Clin Oncol 42 (Suppl 16): S6102-S6102, 2024.
10. Gao M, Hao Y, Huang MX, Ma DQ, Luo HY, Gao Y, Peng X and Yu GY: Clinicopathological study of distant metastases of salivary adenoid cystic carcinoma. Int J Oral Maxillofac Surg 42: 923-928, 2013.
11. Jang S, Patel PN, Kimple RJ and McCulloch TM: Clinical outcomes and prognostic factors of adenoid cystic carcinoma of the head and neck. Anticancer Res 37: 3045-3052, 2017.
12. Fang Y, Peng Z, Wang Y, Gao K, Liu Y, Fan R, Zhang H, Xie Z and Jiang W: Current opinions on diagnosis and treatment of adenoid cystic carcinoma. Oral Oncol 130: 105945, 2022.
13. Walker M, Dewald A, Refaey A, Berezowski I, Newman J, Younes M and Gray S: Salivary gland adenoid cystic carcinoma presenting as a large metastatic hepatic mass: A case report. J Med Case Rep 19: 126, 2025.
14. Brincat SD and Cassar N: Solitary liver metastasis from adenoid cystic carcinoma of the submandibular gland. BMJ Case Rep 17: e258923, 2024.
15. Li XH, Zhang YT and Feng H: Liver metastasis as the initial clinical manifestation of sublingual gland adenoid cystic carcinoma: A case report. World J Clin Cases 9: 5238-5244, 2021.
16. Spolverato G, Fite J, Bishop J, Argani P and Pawlik TM: Liver metastasis as the initial presentation of adenoid cystic carcinoma. Dig Dis Sci 59: 2004-2006, 2014.
17. Garg N, Tomar R, Goyal S and Singh UR: Isolated liver metastases in an adenoid cystic carcinoma of the submandibular gland on fine needle aspiration cytology: An unusual presentation. Cytopathology 25: 137-138, 2014.
18. Karatzas A, Katsanos K, Maroulis I, Kalogeropoulou C, Tzorakoleftherakis E and Karnabatidis D: Multi-modality curative treatment of salivary gland cancer liver metastases with drug-eluting bead chemoembolization, radiofrequency ablation, and surgical resection: A case report. J Med Case Rep 5: 416, 2011.
19. Deshpande AH and Kelkar AA: Hepatic metastasis as an initial manifestation of salivary adenoid cystic carcinoma: Cytologic diagnosis. Diagn Cytopathol 37: 45-47, 2009.
20. Zhou M, Ma T, Wang X, Zhang S, Yang G, Song R and Chen X: High-risk subtype: Clinical manifestations and molecular characteristics of submandibular gland adenoid cystic carcinoma. Front Oncol 12: 1021169, 2022.
21. Megwalu UC and Sirjani D: Risk of nodal metastasis in major salivary gland adenoid cystic carcinoma. Otolaryngol Head Neck Surg 156: 660-664, 2017.
22. Tasoulas J, Divaris K, Theocharis S, Farquhar D, Shen C, Hackman T and Amelio AL: Impact of tumor site and adjuvant radiotherapy on survival of patients with adenoid cystic carcinoma: A SEER database analysis. Cancers (Basel) 13: 589, 2021.

23. Mishra R, Patel H, Alanazi S, Kilroy MK and Garrett JT: PI3K inhibitors in cancer: Clinical implications and adverse effects. Int J Mol Sci 22: 3464, 2021.
24. Ren Y, Hong Y, He W, Liu Y, Chen W, Wen S and Sun M: EGF/EGFR promotes salivary adenoid cystic carcinoma cell malignant neural invasion via activation of PI3K/AKT and MEK/ERK signaling. Curr Cancer Drug Targets 22: 603-616, 2022.
25. Wang C, Zhang Y, Zhang Y and Li B: A bibliometric analysis of gastric cancer liver metastases: Advances in mechanisms of occurrence and treatment options. Int J Surg 110: 2288-2299, 2024.
26. Geiger JL, Ismaila N, Beadle B, Caudell JJ, Chau N, Deschler D, Glastonbury C, Kaufman M, Lamarre E, Lau HY, *et al*: Management of salivary gland malignancy: ASCO guideline. J Clin Oncol 39: 1909-1941, 2021.
27. Locati LD, Bossi P, Perrone F, Potepan P, Crippa F, Mariani L, Casieri P, Orsenigo M, Losa M, Bergamini C, *et al*: Cetuximab in recurrent and/or metastatic salivary gland carcinomas: A phase II study. Oral Oncol 45: 574-578, 2009.
28. Agulnik M, Cohen EWE, Cohen RB, Chen EX, Vokes EE, Hotte SJ, Winquist E, Laurie S, Hayes DN, Dancey JE, *et al*: Phase II study of lapatinib in recurrent or metastatic epidermal growth factor receptor and/or erbB2 expressing adenoid cystic carcinoma and non-adenoid cystic carcinoma malignant tumors of the salivary glands. J Clin Oncol 25: 3978-3984, 2007.
29. Guigay J, Fayette J, Even C, Cupissol D, Rolland F, Peyrade F, Laguerre B, Le Tourneau C, Zanetta S, Le Moal LB, *et al*: PACSA: Phase II study of pazopanib in patients with progressive recurrent or metastatic (R/M) salivary gland carcinoma (SGC). J Clin Oncol 34 (Suppl 15): S6086, 2016.
30. Cheung LWT, Yu S, Zhang D, Li J, Ng PK, Panupinthu N, Mitra S, Ju Z, Yu Q, Liang H, *et al*: Naturally occurring neomorphic PIK3R1 mutations activate the MAPK pathway, dictating therapeutic response to MAPK pathway inhibitors. Cancer Cell 26: 479-494, 2014.